

Pion Rescattering in Two-Pion Decay of Heavy Quarkonia

T.A. Lähde^{*} and D.O. Riska[†]

*Helsinki Institute of Physics,
PL 64 University of Helsinki, Finland*

Abstract

The role of pion rescattering in $\pi\pi$ decay of radially excited heavy quarkonia modeled in terms of a $Q\pi\pi$ coupling, is investigated within the framework of the covariant Blankenbecler-Sugar equation. The effects of pion rescattering (or pion exchange) are shown to be large, unless the coupling of the two-pion system to the heavy quarks is mediated by a fairly light scalar σ meson, which couples to the gradients of the pion fields. The Hamiltonian model for the quarkonium states is formed of linear scalar confining, screened one-gluon exchange and instanton induced interaction terms. The widths and energy distributions of the basic decays $\psi' \rightarrow J/\psi \pi\pi$ and $\Upsilon' \rightarrow \Upsilon \pi\pi$ are shown to be satisfactorily described by this model. The implications of this model for the decays of the $\Upsilon(3S)$ state are discussed.

^{*}talahde@pcu.helsinki.fi

[†]riska@pcu.helsinki.fi

1 Introduction

Two pion decay of radially excited heavy quarkonium ($Q\bar{Q}$) states empirically constitutes a significant fraction of their total decay widths [1]. Indeed, in the case of the ψ' (or $\psi(2S)$), the branching ratio of the $\pi\pi$ decay mode is empirically as large as $\sim 50\%$. Consequently, there has been considerable theoretical interest in these decays as the coupling of two pions to heavy flavor mesons (or quarks) involves at least two gluons if not a glueball. A number of different theoretical approaches for the coupling of two-pions to heavy mesons have been proposed, ranging e.g. from effective field theory descriptions [3] and directly QCD-motivated models [4] to phenomenological models [5]. In ref. [6], a Lagrangian motivated by chiral perturbation theory has been fitted to experiment. The current empirical data on the $\pi\pi$ decay of the ψ' and the analogous Υ' (or $\Upsilon(2S)$) state, along with a review of the relevant literature on the subject is given in ref. [2].

Theoretical work on the $\pi\pi$ decays of excited heavy quarkonia has demonstrated that the empirical energy spectra of the emitted two-pion system demands that the pions be derivatively coupled to the heavy quarkonium states. This is consistent with the role of the pions as Goldstone bosons of the spontaneously broken approximate chiral symmetry of QCD. Most models [3, 4, 5, 6] have dealt with the coupling of two-pions to the heavy meson as a whole rather than to its constituent quarks. The satisfactory description obtained suggests that the decay amplitude T_{fi} at the quark level should be a smoothly varying, almost constant, function of the two-pion momentum \vec{q} , which is dominated by single-quark mechanisms for two-pion emission.

At the quark level, this is, however, not *a priori* expected to be the case. In the non-relativistic approximation, the amplitude for $\pi\pi$ decay of excited S -wave states to the ground state through single-quark mechanisms is small because of the orthogonality of the quarkonium wave functions for different states. In this approximation the hadronic matrix element does not lead to a constant decay amplitude, but to one that increases quadratically with the two-pion momentum \vec{q} . Furthermore, the pion rescattering or pion exchange term that appears naturally as a consequence of the coupling of two-pions to constituent quarks is in contrast not suppressed by the orthogonality of the wave functions, and may actually be shown to be dominant even in the relativistic case.

It is shown here that an unrealistically large pion exchange contribution may be avoided if the $Q\pi\pi$ vertex involves an intermediate, fairly light and broad σ meson, in line with the phenomenological resonance model of ref. [5]. An intermediate σ meson leads to a drastic reduction of the contributions from pion exchange mechanisms, while single quark amplitudes are but slightly affected. This can be understood qualitatively as a consequence of the exchanged pion being off shell. The relativistic treatment of the quark spinors is shown to lead to a significant strengthening of the single quark amplitudes relative to those of pion exchange, and also reproduces the expected smooth behavior of the decay amplitude.

The wave functions of the heavy quarkonium states are here obtained as solutions to the covariant Blankenbecler-Sugar (BSLT) equation [7, 8] with an interaction Hamiltonian, which consists of the scalar linear confining + screened one-gluon exchange (OGE) model of ref. [9] and the instanton model employed in refs. [10, 11].

A fairly satisfactory description of the empirical $\pi\pi$ decay rates and spectra for the transitions $\psi(2S) \rightarrow J/\psi \pi\pi$ and $\Upsilon(2S) \rightarrow \Upsilon(1S)\pi\pi$ is achieved when the pion rescattering contribution is small. The decay $\Upsilon(3S) \rightarrow \Upsilon(1S)\pi\pi$ remains something of a puzzle, as the spectrum of the two-pion for this transition indicates a dominance of the rescattering contribution.

This paper is organized as follows: Section 2 describes the interaction Hamiltonian of the $Q\bar{Q}$ system as employed with the BSLT equation and the resulting spectra and wave functions of the $Q\bar{Q}$ states. Section 3 contains the calculation of the $\pi\pi$ width and the derivation of the decay amplitude T_{fi} and the hadronic matrix elements. In section 4 the results for the $\pi\pi$ decays of the ψ' and Υ' states are presented. Section 5 contains a discussion of the obtained results for the $\pi\pi$ decays of these states along with remarks on the implications of this model for the $\pi\pi$ decays of the $\Upsilon(3S)$ state.

2 Interaction Hamiltonian for $Q\bar{Q}$ Systems

2.1 Model Hamiltonian

The interaction Hamiltonian used in this paper in conjunction with the covariant Blankenbecler-Sugar (BSLT) equation to obtain spectra and wave functions for the charmonium ($c\bar{c}$) and bottomonium ($b\bar{b}$) states may be expressed as

$$H_{\text{int}} = V_{\text{conf}} + V_{\text{OGE}} + V_{\text{inst}}, \quad (1)$$

where the different parts denote the confining interaction, one-gluon exchange (OGE) and instanton induced interactions respectively. In view of the indications given by the radiative M1 transitions in heavy quarkonia [12] as well as the M1 [9] and pion [13, 14] decays of the heavy-light mesons, the confining interaction is here taken to couple as a Lorentz scalar. The OGE interaction motivated by perturbative QCD has vector coupling structure. In the nonrelativistic approximation the interaction potentials in the Hamiltonian (1) may be expressed in the form:

$$V_{\text{conf}} = cr - \frac{c}{r} \frac{M_Q^2 + M_{\bar{Q}}^2}{4M_Q^2 M_{\bar{Q}}^2} \vec{S} \cdot \vec{L} \quad (2)$$

for the scalar confining interaction, where the constant c is known [12, 15, 19] to be of the order ~ 1 GeV/fm. The second term in eq. (2) represents the spin-orbit component of the confining interaction. Note that the antisymmetric spin-orbit interaction will be omitted throughout since it vanishes in the case of equal quark and antiquark masses. Similarly, the OGE interaction may be expressed as [16]

$$\begin{aligned} V_{\text{OGE}} = & -\frac{4}{3} \frac{\alpha_s}{r} + \frac{2}{3} \frac{\alpha_s}{r^3} \left(\frac{M_Q^2 + M_{\bar{Q}}^2}{2M_Q^2 M_{\bar{Q}}^2} + \frac{2}{M_Q M_{\bar{Q}}} \right) \vec{S} \cdot \vec{L} + \frac{8\pi}{9} \frac{\alpha_s}{M_Q M_{\bar{Q}}} \delta^3(r) \vec{\sigma}_Q \cdot \vec{\sigma}_{\bar{Q}} \\ & + \frac{1}{3} \frac{\alpha_s}{M_Q M_{\bar{Q}} r^3} S_{12}, \end{aligned} \quad (3)$$

where α_s denotes the running coupling constant of perturbative QCD, S_{12} is the usual tensor operator $S_{12} = 3(\vec{\sigma}_Q \cdot \hat{r})(\vec{\sigma}_{\bar{Q}} \cdot \hat{r}) - \vec{\sigma}_Q \cdot \vec{\sigma}_{\bar{Q}}$, and $M_Q, M_{\bar{Q}}$ denote the heavy quark and antiquark masses, respectively.

The instanton induced interaction in systems with heavy quarks has been considered in refs. [10, 11] and consists of a spin-independent as well as a $\vec{\sigma}_Q \cdot \vec{\sigma}_{\bar{Q}}$ spin-spin interaction term. However, it was also found that only the spin-independent term contributes significantly for systems composed of two heavy quarks. Thus the instanton contribution to eq. (1) may be expressed as [11]

$$V_{\text{inst}} = -\frac{(\Delta M_Q)^2}{4n} \delta^3(r), \quad (4)$$

where ΔM_Q denotes the mass shift of the heavy constituent quark due to the instanton induced interaction. For a charm quark, this is expected to be of the order of ~ 100 MeV [11]. The parameter n represents the instanton density, which is typically assigned values around $\sim 1 \text{ fm}^{-4}$.

2.2 The Blankenbecler-Sugar equation

The covariant Blankenbecler-Sugar equation for a quark-antiquark system may be expressed as an eigenvalue equation similar to the nonrelativistic Schrödinger equation:

$$\left(-\frac{\vec{\nabla}^2}{2\mu} + V \right) \Psi_{\text{nlim}}(\vec{r}) = \varepsilon \Psi_{\text{nlim}}(\vec{r}). \quad (5)$$

Here μ denotes the reduced mass of the quark-antiquark system, while the eigenvalue ε is related to the energy E of the $Q\bar{Q}$ state as

$$\varepsilon = \frac{[E^2 - (M_Q + M_{\bar{Q}})^2][E^2 - (M_Q - M_{\bar{Q}})^2]}{8\mu E^2}. \quad (6)$$

For equal quark and antiquark masses, this expression simplifies to $(E^2 - 4M_Q^2)/4M_Q$. The relation between the interaction operator V , which in general is nonlocal, to the $Q\bar{Q}$ irreducible quasipotential \mathcal{V} is (in momentum space)

$$V(\vec{p}', \vec{p}) = \sqrt{\frac{M_Q + M_{\bar{Q}}}{W(\vec{p}')}} \mathcal{V}(\vec{p}', \vec{p}) \sqrt{\frac{M_Q + M_{\bar{Q}}}{W(\vec{p})}}, \quad (7)$$

where the function W is defined as

$$W(\vec{p}) = E_Q(\vec{p}) + E_{\bar{Q}}(\vec{p}), \quad (8)$$

with $E_Q(\vec{p}) = \sqrt{M_Q^2 + \vec{p}^2}$. In the Born approximation the quasipotential \mathcal{V} is set equal to the $Q\bar{Q}$ invariant scattering amplitude \mathcal{T} , and thus a constructive relation to field theory obtains.

Comparison of the BSLT equation to the nonrelativistic Schrödinger equation reveals that the quadratic mass operator employed by the former (6) leads to an effective weakening of the repulsive kinetic energy operator. Also, wavefunctions that are solutions to eq. (5), allow retention of the conventional quantum mechanical operator structure. For systems that contain charm quarks the static interaction Hamiltonian described above has but qualitative value, because of the slow convergence of the asymptotic expansion in v/c [9]. Therefore the potentials in eq. (1) should be replaced with versions, which take into account both the modification (7) and the relativistic effects associated with the Lorentz structure of the interaction, as well as the effects of the running coupling $\alpha_s(k^2)$. If the nonlocal effects of quadratic and higher order in $\vec{P} = (\vec{p}' + \vec{p})/2$ are dropped, this may be achieved by replacing the main term of the OGE interaction by [9]

$$V_{\text{OGE}} = -\frac{4}{3} \frac{2}{\pi} \int_0^\infty dk j_0(kr) \frac{M_Q}{e_Q} \frac{M_{\bar{Q}}}{e_{\bar{Q}}} \left(\frac{M_Q + M_{\bar{Q}}}{e_Q + e_{\bar{Q}}} \right) \alpha_s(k^2), \quad (9)$$

where the factors e_Q and $e_{\bar{Q}}$ are defined as

$$e_Q = \sqrt{M_Q^2 + \frac{k^2}{4}}, \quad e_{\bar{Q}} = \sqrt{M_{\bar{Q}}^2 + \frac{k^2}{4}}. \quad (10)$$

For the running QCD coupling $\alpha_s(k^2)$, the parameterization of ref. [17]:

$$\alpha_s(k^2) = \frac{12\pi}{27} \frac{1}{\ln[(k^2 + 4m_g^2)/\Lambda_0^2]}. \quad (11)$$

has been employed. Here Λ_0 and m_g are parameters that determine the high- and low-momentum transfer behavior of α_s respectively, which will be determined by a fit to the experimental heavy quarkonium spectra. With exception of the effects of the running coupling α_s , which lead to a strengthening of the long-range part of the OGE interaction, the relativistic modifications in eq. (9) lead to a strong suppression of the short-range Coulombic potential. These relativistic modifications are however significant only for distances < 0.5 fm. In principle, a relativistic form for the linear scalar confining interaction

analogous to eq. (9) may also be constructed, but in view of its long-range nature the resulting modifications are less significant. A similar modification of the spin-orbit potentials associated with the OGE and confining interactions gives

$$V_{\text{OGE}}^{\text{LS}} = \frac{2}{3\pi r} \vec{S} \cdot \vec{L} \int_0^\infty dk k j_1(kr) \left(\frac{M_Q + M_{\bar{Q}}}{e_Q + e_{\bar{Q}}} \right) \left(\frac{e_Q + M_Q}{e_Q} \right) \left(\frac{e_{\bar{Q}} + M_{\bar{Q}}}{e_{\bar{Q}}} \right) \\ \left\{ \frac{1}{(e_{\bar{Q}} + M_{\bar{Q}})^2} \left[1 - \frac{k^2}{4(e_Q + M_Q)^2} \right] + \frac{1}{(e_Q + M_Q)^2} \left[1 - \frac{k^2}{4(e_{\bar{Q}} + M_{\bar{Q}})^2} \right] \right. \\ \left. + \frac{4}{(e_Q + M_Q)(e_{\bar{Q}} + M_{\bar{Q}})} \right\} \alpha_s(k^2) \quad (12)$$

for the OGE spin-orbit interaction, and

$$V_{\text{conf}}^{\text{LS}} = -\frac{2}{\pi} \frac{c}{r} \vec{S} \cdot \vec{L} \int_0^\infty dk \frac{j_1(kr)}{k} \left(\frac{M_Q + M_{\bar{Q}}}{e_Q + e_{\bar{Q}}} \right) \left(\frac{1}{e_Q(e_Q + M_Q)} + \frac{1}{e_{\bar{Q}}(e_{\bar{Q}} + M_{\bar{Q}})} \right) \quad (13)$$

for the confinement spin-orbit interaction. In order to obtain eq. (13), the Fourier transform of the linear confining interaction was taken to be

$$V_{\text{conf}}(k, \lambda) = \lim_{\lambda \rightarrow 0} 8\pi c \left(\frac{4\lambda^2}{(\lambda^2 + k^2)^3} - \frac{1}{(\lambda^2 + k^2)^2} \right), \quad (14)$$

which for the purpose of calculating the spin-orbit contribution may be directly simplified to

$$V_{\text{conf}}(k) = -\frac{8\pi c}{k^4}. \quad (15)$$

Note that eqs. (12) and (13) are free of singularities that have to be treated in first order perturbation theory, particularly the r^{-3} singularity of the OGE spin-orbit interaction which is an illegal operator in the differential equation (5). The modification of the spin-spin delta function term in eq. (3) is obtained as

$$V_{\text{OGE}}^{\text{SS}} = \frac{4}{9\pi} \vec{\sigma}_Q \cdot \vec{\sigma}_{\bar{Q}} \int_0^\infty dk k^2 j_0(kr) \left(\frac{M_Q + M_{\bar{Q}}}{e_Q + e_{\bar{Q}}} \right) \frac{\alpha_s(k^2)}{e_Q e_{\bar{Q}}} \quad (16)$$

and that of the tensor interaction as

$$V_{\text{OGE}}^{\text{T}} = \frac{2}{9\pi} S_{12} \int_0^\infty dk k^2 j_2(kr) \left(\frac{M_Q + M_{\bar{Q}}}{e_Q + e_{\bar{Q}}} \right) \frac{\alpha_s(k^2)}{e_Q e_{\bar{Q}}}. \quad (17)$$

These forms are also free of singularities that have to be treated in first order perturbation theory. Note that for $r > 0.5$ fm the modified potentials asymptotically approach the static forms of eqs. (2) and (3), if α_s is taken to be constant. In case of the instanton induced interaction, the delta function of eq. (4) is modified as

$$V_{\text{inst}} = -\frac{(\Delta M_Q)^2}{4n} \int_0^\infty dk k^2 j_0(kr) \left(\frac{M_Q + M_{\bar{Q}}}{e_Q + e_{\bar{Q}}} \right) \frac{M_Q M_{\bar{Q}}}{e_Q e_{\bar{Q}}}, \quad (18)$$

leading to a smeared out form of the delta function, which allows for a direct numerical treatment of the instanton potential. In the limit of very large quark and antiquark masses (the static limit) the above equation reduces to the form (4).

2.3 Heavy Quarkonium Spectra and Wave functions

The heavy quark masses and the parameters in the quark-antiquark interaction operator are determined by a fit to the empirical charmonium and bottomonium spectra, which was achieved by numerical solution of eq. (5) for the quarkonium states with the Runge-Kutta-Nyström (RKN) algorithm. The resulting spectra are presented in Fig. 1 and the reduced radial wave functions corresponding to the $1S$ and $2S$ states of charmonium and bottomonium are shown in Fig. 2.

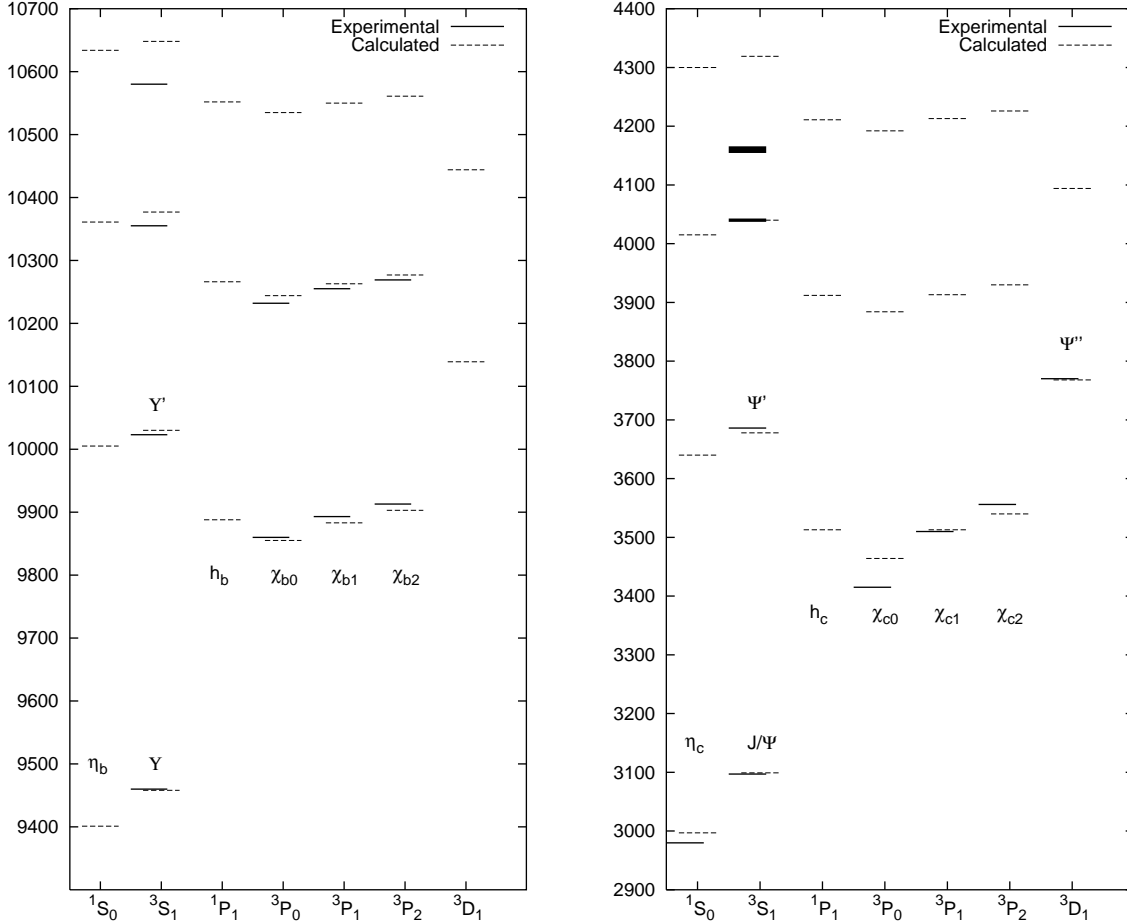


Figure 1: Calculated and experimental Bottomonium($b\bar{b}$) and Charmonium($c\bar{c}$) spectra. All states are given in MeV, and correspond to the data in Table 1. The thickness of the lines denoting the experimentally determined states indicate the uncertainty in the mass of the state. Note that the identification of the 4^3S_1 state in charmonium is uncertain, and may actually be a 2^1D_2 state, or a mixture of the two. The threshold for $D\bar{D}$ decay is at ~ 3750 MeV, and for $B\bar{B}$ decay at ~ 10500 MeV.

$n^{2S+1}L_J$	$b\bar{b}$	Exp($b\bar{b}$)	$c\bar{c}$	Exp($c\bar{c}$)
1^1S_0	9401	–	2997	2980 ± 1.8
2^1S_0	10005	–	3640	–
3^1S_0	10361	–	4015	–
4^1S_0	10634	–	4300	–
1^3S_1	9458	9460	3099	3097
2^3S_1	10030	10023	3678	3686
3^3S_1	10377	10355	4040	4040 ± 10
4^3S_1	10648	10580	4319	4159 ± 20 ?
1^1P_1	9888	–	3513	–
2^1P_1	10266	–	3912	–
3^1P_1	10552	–	4211	–
1^3P_0	9855	9860	3464	3415
2^3P_0	10244	10232	3884	–
3^3P_0	10535	–	4192	–
1^3P_1	9883	9893	3513	3511
2^3P_1	10263	10255	3913	–
3^3P_1	10550	–	4213	–
1^3P_2	9903	9913	3540	3556
2^3P_2	10277	10269	3930	–
3^3P_2	10561	–	4226	–
1^3D_1	10139	–	3768	3770 ± 2.5
2^3D_1	10444	–	4094	– ?

Table 1: Calculated and experimental charmonium and bottomonium states rounded to the nearest MeV. The experimental states correspond to the values reported by ref. [1]. The states are classified according to excitation number n , total spin S , total orbital angular momentum L and total angular momentum J . These values are plotted in Fig. 1. Experimental uncertainties are indicated only where they are appreciable.

The calculated states listed in Table 1 are, for the most part, in good agreement with the experimental results. The agreement is similar to that achieved in ref. [18] as well as in ref. [15], where the heavy quark potential was determined by numerical lattice QCD calculation. The threshold for $D\bar{D}$ fragmentation in charmonium lies at ~ 3750 MeV, while that for $B\bar{B}$ fragmentation in bottomonium lies at ~ 10500 MeV. The states that lie above the threshold for strong decay are less well described by the present model, a feature that is shared with other similar models, e.g. ref. [18]. Below threshold, the most significant discrepancy is the too small hyperfine splittings obtained for the $L = 1$ states in charmonium. This problem appears to be common for all calculations based on interaction Hamiltonians formed of OGE + scalar confinement components [15, 19, 18]. Here this problem may be traced to the weakness of the OGE tensor interaction as given by eqs. (3) and (17).

The coupling constants used in the interaction Hamiltonian were optimized by fits to the empirical charmonium and bottomonium spectra, and are listed in Table 2. In order to accommodate universal parameters for the OGE and linear confining interactions, perfect agreement with experiment had to be sacrificed in the bottomonium sector. The resulting central (spin-independent) components of the quark-antiquark potential is shown in Fig. 3 for the parameters of Table 2. They turn out to be quite well described by a Cornell form $V(r) = -a/r + cr + b$, with a Coulombic part that is somewhat stronger for the charmonium system.

Parameter	Current value	Other sources
M_b	4885 MeV	4870 MeV [18]
M_c	1500 MeV	1530 MeV [18]
Λ_{QCD}	260 MeV	200-300 MeV [17]
m_g	290 MeV	$m_g > \Lambda_{\text{QCD}}$ [17]
c	890 MeV/fm	912 MeV/fm [18]
$\frac{(\Delta M_c)^2}{4n}$	0.084 fm ⁻⁶	~ 0.05 fm ⁻⁶ [11]
$\frac{(\Delta M_b)^2}{4n}$	0.004 fm ⁻⁶	?

Table 2: Quark masses and coupling constants corresponding to the calculated spectra in Fig. 1. The heavy masses are close to those used in ref. [18], and in general in agreement with the values in earlier work. The values of Λ_{QCD} and m_g are also in line with the general criteria of ref. [17]. The resulting parameterization of the strong coupling α_s is shown in Fig. 4. The confining interaction strength c is also in good agreement with the values of earlier calculations [18, 19]. For charmonium, the strength of the instanton induced interaction is comparable to the estimate given by ref. [11].

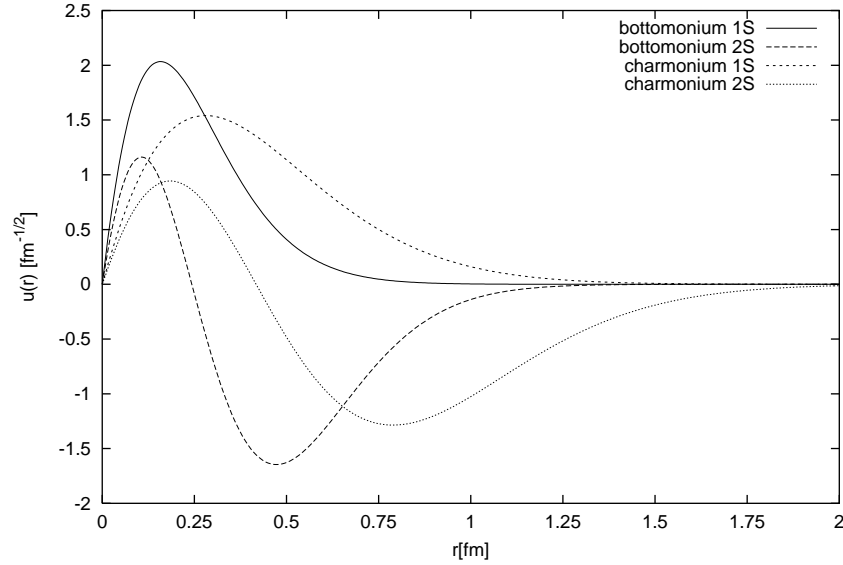


Figure 2: Reduced radial wave functions $u(r) = r\psi(r)$ for the Υ , Υ' , J/ψ and ψ' states, corresponding to the interaction Hamiltonian described in section 2.2.

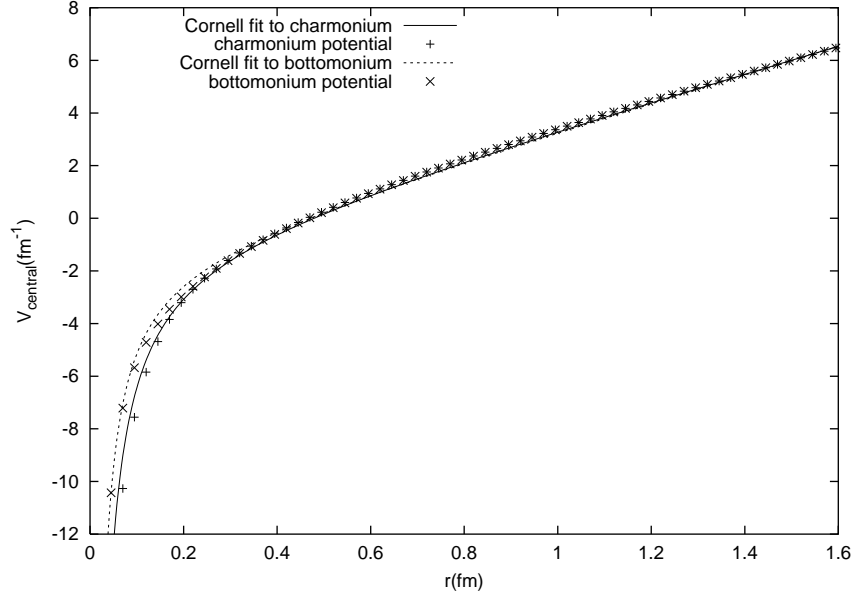


Figure 3: Plot of calculated central components of the $Q\bar{Q}$ potentials together with Cornell type best fits, $V(r) = -a/r + cr + b$. For charmonium, the parameters are $a = 0.570888$, $b = -1.24528 \text{ fm}^{-1}$, $c = 5.08521 \text{ fm}^{-2}$, and for bottomonium $a = 0.407118$, $b = -1.61144 \text{ fm}^{-1}$, $c = 5.24625 \text{ fm}^{-2}$.

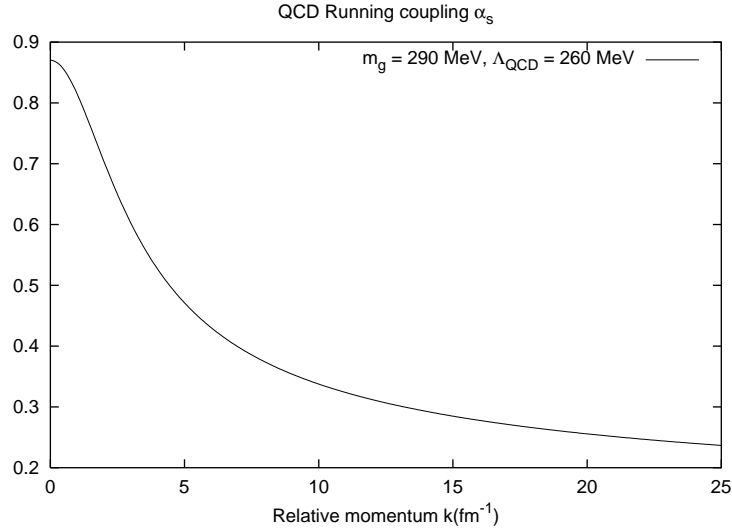


Figure 4: Plot of α_s with the parameters employed in this paper. Here $\alpha_s \sim 0.38$ at the charmonium scale ($\sim 1500 \text{ MeV}$) and $\alpha_s \sim 0.25$ at the bottomonium scale ($\sim 4800 \text{ MeV}$). The present form also agrees quite well with the low momentum limit of $\alpha_s/\pi \sim 0.26$ suggested in ref. [17].

3 The Model for $\pi\pi$ decay

3.1 Width for $\pi\pi$ decay

The general expression for the two pion decay width of an excited $Q\bar{Q}$ meson may be written in the form

$$\Gamma = (2\pi)^4 \int \frac{d^3k_a}{(2\pi)^3} \frac{d^3k_b}{(2\pi)^3} \frac{d^3P_f}{(2\pi)^3} \frac{M_f M_i}{E_f E_i} \frac{|T_{fi}|^2}{4\omega_a \omega_b} \delta^{(4)}(P_f + k_a + k_b - P_i). \quad (19)$$

Here k_a and k_b denote the four-momenta of the two emitted pions, P_i and P_f those of the initial and final state $Q\bar{Q}$ mesons while ω_a and ω_b denote the energies of the emitted pions respectively. The factors M/E are normalization factors for the heavy meson states similar to those employed in ref. [14]. Since the constituents of the $Q\bar{Q}$ mesons form bound states, their normalization factors are included in the spinors $\bar{u}(p')$ and $u(p)$ in eq. (29). In the laboratory frame $P_i^0 = E_i = M_i$. By introducing the variables $\vec{Q} = (\vec{k}_b - \vec{k}_a)/2$ and $\vec{q} = \vec{k}_b + \vec{k}_a$, the decay width expression may be rewritten as

$$\Gamma = \int \frac{d^3q d^3Q}{(2\pi)^5} \frac{M_f}{E_f} \frac{|T_{fi}|^2}{4\omega_a \omega_b} \delta\left(\sqrt{q^2 + M_f^2} + \omega_a + \omega_b - M_i\right). \quad (20)$$

Here the pion energy factors are defined as $\omega_a = \sqrt{m_\pi^2 + (\vec{q}/2 - \vec{Q})^2}$ and $\omega_b = \sqrt{m_\pi^2 + (\vec{q}/2 + \vec{Q})^2}$ respectively. The remaining delta function determines the variable \vec{Q} , so that finally the expression for the differential width becomes

$$\frac{d\Gamma}{d\Omega_q} = \frac{1}{4} \frac{1}{(2\pi)^4} \int_0^{q_f} dq q^2 \int_{-1}^1 dz \frac{Q_f^2(q, z)}{\omega_a(q, z) (Q_f + \frac{qz}{2}) + \omega_b(q, z) (Q_f - \frac{qz}{2})} \frac{M_f}{E_f(q)} |T_{fi}|^2. \quad (21)$$

In eq. (21), the variable z is defined by $\vec{Q} \cdot \vec{q} = Q_f q z$, and E_f denotes the energy of the final state $Q\bar{Q}$ meson and is given by $E_f = \sqrt{q^2 + M_f^2}$. With this notation the pion energies ω_a and ω_b are given by the expressions

$$\omega_a = \sqrt{m_\pi^2 + Q_f^2 + q^2/4 - Q_f q z} \quad \text{and} \quad \omega_b = \sqrt{m_\pi^2 + Q_f^2 + q^2/4 + Q_f q z}, \quad (22)$$

where the fixed variable Q_f is given by

$$Q_f^2 = \frac{(E_f - M_i)^4 - (4m_\pi^2 + q^2)(E_f - M_i)^2}{4(E_f - M_i)^2 - 4q^2 z^2}. \quad (23)$$

In the expressions above, m_π denotes the pion mass. Since different charge states are considered in this paper, slightly different pion masses will be used for decays that involve charged or neutral pions. The integration limit q_f corresponds to the maximal momentum of any one of the final state particles, e.g. the final state $Q\bar{Q}$ meson. Thus q_f corresponds to the q-value of a decay of the form $A' \rightarrow AX$, where A' and A are the appropriate $Q\bar{Q}$ meson states and X is a particle with mass $M_X = 2m_\pi$. The appropriate values of q_f for the different decays are listed in Table 3.

The above equations are ideally suited for computation of the $\pi\pi$ decay width using a hadronic matrix element T_{fi} . However, experimental data is usually presented [2] in terms of a dimensionless variable x , which is defined as

$$x = \frac{m_{\pi\pi} - 2m_\pi}{\Delta M}. \quad (24)$$

Here $m_{\pi\pi}$ denotes the invariant mass $\sqrt{s_{\pi\pi}}$ of the two-pion system, and $\Delta M = M_i - M_f - 2m_\pi$. With these definitions, the variable x is always between 0 and 1. The relation between q and $m_{\pi\pi}$ may then be obtained as [1]

$$|\vec{q}| = \frac{\sqrt{(M_i^2 - (M_f + m_{\pi\pi})^2)(M_i^2 - (M_f - m_{\pi\pi})^2)}}{2M_i}. \quad (25)$$

From this relation, the Jacobian of transformation may be obtained as

$$\frac{dq}{dx} = \frac{\Delta M}{4M_i^2 q(m_{\pi\pi})} \{ [M_i^2 - (M_f + m_{\pi\pi})^2] (M_f - m_{\pi\pi}) - [M_i^2 - (M_f - m_{\pi\pi})^2] (M_f + m_{\pi\pi}) \}. \quad (26)$$

Finally the total decay width may be calculated as

$$\Gamma = \int_0^{q_f} dq \frac{d\Gamma}{dq} = - \int_0^1 dx \frac{d\Gamma}{dq} \frac{dq}{dx}, \quad (27)$$

where the minus sign appears because the integration limits have been reversed to take into account the fact that $q = q_f$ corresponds to $x = 0$. In eq. (27), the latter form turns out to be the most convenient since experiments generally present the measurements of the $\pi\pi$ energy distribution using dimensionless quantities, e.g. by plotting $1/\Gamma(d\Gamma/dx)$ versus x . In the following section, the model for the $\pi\pi$ decay amplitude is presented.

3.2 Amplitude for $\pi\pi$ decay

There are several different models for the coupling of two-pions to heavy constituent quarks. The emission of two-pions from a heavy flavor quark is mediated by two or more gluons or a glueball. For small momenta of the two-pion system this coupling may be approximated by a point coupling, but at larger momenta the strong interaction between the pions has to be taken into account, e.g. approximately through a broad scalar meson resonance.

If the coupling of the pions to the constituent quark does not involve derivatives of the pion field, agreement with experiment is excluded for the pion invariant mass distributions in the decays $\Upsilon' \rightarrow \Upsilon \pi\pi$ and $\psi' \rightarrow J/\psi \pi\pi$ [2, 5]. Derivative couplings for the pions are also consistent with the role of pions as Goldstone bosons of the spontaneously broken approximate chiral symmetry of QCD. The model for the $Q\pi\pi$ interaction Lagrangian is therefore expected to have the form

$$\mathcal{L}_{Q\pi\pi} = 4\pi\lambda \bar{\psi}_Q (\partial_\mu \vec{\phi}_\pi) \cdot (\partial_\mu \vec{\phi}_\pi) \psi_Q, \quad (28)$$

where λ is a coupling constant of dimension $[\text{MeV}]^{-3}$ and $\psi_Q, \bar{\psi}_Q$ denote the heavy quark spinors.

Since the above Lagrangian couples the two-pions directly to the constituent quarks of the heavy meson, pion exchange mechanisms describing rescattering of the emitted pions appear as a natural consequence, in addition to the single-quark mechanisms. The relevant Feynman diagrams are shown in Fig. 5. The amplitude T_{fi} in eq. (21) may thus be expressed in the form

$$T = T_Q + T_{\bar{Q}} + T_{\text{ex}} + T_{\text{exc}}, \quad (29)$$

where the amplitudes T_Q and $T_{\bar{Q}}$ are single quark amplitudes describing two-pion emission from the quark and antiquark respectively. For the equal mass quarkonia considered here, these two amplitudes are identical. The amplitudes T_{ex} and T_{exc} describe diagrams where a pion is exchanged between the quark and antiquark during the decay process. T_{exc} differs from T_{ex} by an interchange of the emitted pions, which will be shown to make only a very small difference. The isospin dependence of the coupling (28) implies that

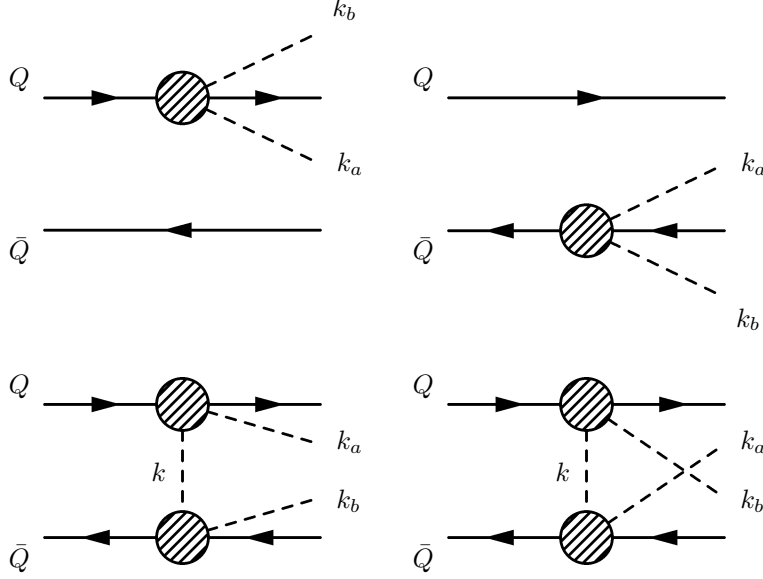


Figure 5: Feynman diagrams for the emission of two-pions by heavy constituent quarks. The two upper diagrams correspond to the single-quark amplitudes T_Q and $T_{\bar{Q}}$ respectively, while the two lower diagrams describe the pion exchange (or pion rescattering) amplitude T_{ex} and the crossed amplitude T_{exc} .

$$|T|_{\pi\pi}^2 = 2|T|_{\pi^+\pi^-}^2 + |T|_{\pi^0\pi^0}^2. \quad (30)$$

As a consequence the width for decay to charged pions should be twice that for decay to neutral pions. This is in fair agreement with what is found experimentally [1, 2]. Averaging over initial spin states and summing over final spin states introduces nothing further, since only the parts of the amplitudes in Fig. 5 that are spin independent contribute significantly to the decay widths. Treating the Feynman diagrams of Fig. 5 similarly as the pointlike Weinberg-Tomozawa interaction for light constituent quarks [20], then the following expression describing the single quark diagrams are obtained:

$$T_{1q} = T_Q + T_{\bar{Q}} = -2 \cdot 8\pi\lambda \, k_a \cdot k_b \, \mathcal{M}_{1q}, \quad (31)$$

where k_a and k_b are the four-momenta of the emitted pions, and \mathcal{M}_{1q} is a matrix element involving the initial and final state wave functions and quark spinors. Similarly, the amplitude corresponding to the pion-exchange diagrams may be obtained (in momentum space) as

$$T_{2q} = T_{\text{ex}} + T_{\text{exc}} = -2 \cdot (8\pi\lambda)^2 \frac{k_a \cdot k \, k_b \cdot k}{k^2 + m_\pi^2}. \quad (32)$$

In eq. (32), the expression $k_a \cdot k \, k_b \cdot k$ may be written in the form

$$k_a \cdot k \, k_b \cdot k = \frac{\vec{k}_a \cdot \vec{k}_b \, \vec{k}^2}{3} + \left[\vec{k}_a \cdot \vec{k} \, \vec{k}_b \cdot \vec{k} - \frac{\vec{k}_a \cdot \vec{k}_b \, \vec{k}^2}{3} \right] - \vec{k}_a \cdot \vec{k} \, \omega_b k_0 - \vec{k}_b \cdot \vec{k} \, \omega_a k_0 + \omega_a \omega_b k_0^2. \quad (33)$$

If only the S -wave pion production terms (i.e. the first term on the r.h.s. of the above equation and the

term proportional to k_0^2) are retained, eq. (32) may be expressed as

$$T_{2q} = -2 \cdot (8\pi\lambda)^2 \left\{ \frac{1}{3} \left(\frac{\vec{q}^2}{4} - Q_f^2 \right) \left[1 - \frac{A^2}{k^2 + A^2} \right] + \frac{\omega_a \omega_b}{4} (\omega_a - \omega_b)^2 \frac{1}{k^2 + A^2} \right\}, \quad (34)$$

where $A = \sqrt{m_\pi^2 - k_0^2}$. Here k_0 denotes the time component of k . In eq. (34), the left-hand term will, upon Fourier transformation, contain a delta function. Thus, although eq. (32) is formally of second order in λ , it may actually be numerically significantly larger than the single quark amplitude given by eq. (31), if bare vertices are assumed for the $Q\pi\pi$ coupling. Since the kinematical factors associated with the pion exchange amplitude differ from that of the single quark amplitude, dominant pion exchange does not agree with earlier studies [4, 5, 6], which achieved fair agreement with experimental spectra with effectively single-quark amplitudes alone. The indications both from earlier studies of the $2S \rightarrow 1S \pi\pi$ decays and experiment [2] are therefore that the contribution from pion-exchange diagrams should be small. The task here is therefore to attempt an explanation for this experimental feature.

The effect of the strong interaction between two pions in the S -wave $\pi\pi$ may be approximately accounted for by inclusion of an intermediate scalar meson (σ or glueball) resonance in the vertex. This is brought about by modification of the coupling constant λ with a relativistic Breit-Wigner-like scalar meson propagator:

$$\lambda \rightarrow \lambda \left(\frac{M_\sigma^2 + \Gamma_\sigma^2/4}{M_\sigma^2 + q^2 + \Gamma_\sigma^2/4} \right). \quad (35)$$

Here M_σ denotes the pole position $m_\sigma - i\Gamma_\sigma/2$ of the effective scalar meson and q the four-momentum of the scalar meson (σ) resonance. If the variables defined in section 3.1 are employed, the modifications affecting the single-quark amplitude (31) are relatively straightforward. However, the pion-exchange amplitude (32) becomes much more complicated, which is illustrated in Fig. 6:

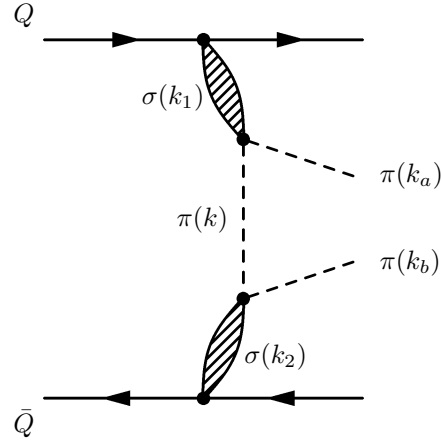


Figure 6: Pion exchange diagram for $\pi\pi$ decay with $Q\pi\pi$ vertices modeled with intermediate heavy σ mesons. Here the σ meson 4-momenta are defined as $k_1 = -k - k_a$ and $k_2 = k - k_b$. Note that just as in Fig. 5, there is also a diagram with k_a and k_b interchanged.

When the modification (35) is taken into account, the expression for the single-quark amplitude (31) becomes

$$T_{1q} = -2 \cdot 8\pi\lambda \left(\frac{M_\sigma^2 + \Gamma_\sigma^2/4}{M_\sigma^2 + q^2 + \Gamma_\sigma^2/4} \right) \left[m_\pi^2 - \frac{1}{2} ((\omega_a + \omega_b)^2 - \vec{q}^2) \right] \mathcal{M}_{1q}. \quad (36)$$

In case of the above single-quark amplitude, the nonrelativistic approximation for the matrix element \mathcal{M}_{1q} cannot be expected to be reliable, even though the quark masses are large. A relativistic form for the matrix element \mathcal{M}_{1q} may be obtained as

$$\mathcal{M}_{1q}^{\text{rel}} = \frac{1}{\pi} \int_0^\infty dr' r' u_f(r') \int_0^\infty dr r u_i(r) \int_0^\infty dP P^2 \int_{-1}^1 dv \alpha(P, v, q)$$

$$j_0 \left(r' \sqrt{P^2 + \frac{q^2}{16} - \frac{Pqv}{2}} \right) j_0 \left(r' \sqrt{P^2 + \frac{q^2}{16} - \frac{Pqv}{2}} \right), \quad (37)$$

where $\alpha(P, v, q)$ is a factor which includes the quark spinors in the coupling (28),

$$\alpha(P, v, q) = \sqrt{\frac{(E + M_Q)(E' + M_Q)}{4EE'}} \left(1 - \frac{P^2 - \vec{q}^2/4}{(E' + M_Q)(E + M_Q)} \right), \quad (38)$$

where the quark energy factors are defined as

$$E = \sqrt{M_Q^2 + P^2 + Pqv + \vec{q}^2/4}, \quad E' = \sqrt{M_Q^2 + P^2 - Pqv + \vec{q}^2/4}. \quad (39)$$

If the nonrelativistic limit is nevertheless employed, eq. (37) reduces to

$$\mathcal{M}_{1q}^{\text{nr}} = \int_0^\infty dr u_f(r) u_i(r) j_0 \left(\frac{qr}{2} \right). \quad (40)$$

In principle the quark spinors in the coupling (28) also contain a spin dependent part that is proportional to $\vec{q} \times \vec{P}$. For the present purposes that contribution turns out to be very tiny and may be safely neglected. It will be shown in the next section that the relativistic modifications to the single-quark matrix element lead to a significant increase of the single quark amplitudes for $\pi\pi$ decay and are important for obtaining agreement with the experimental results.

The pion exchange amplitude corresponding to Fig. 6 may be expressed as

$$T_{\text{ex}} = -(8\pi\lambda)^2 (M_\sigma^2 + \Gamma_\sigma^2/4)^2 \frac{k_a \cdot k \, k_b \cdot k}{(k_1^2 + M_\sigma^2 + \Gamma_\sigma^2/4)(k^2 + m_\pi^2)(k_2^2 + M_\sigma^2 + \Gamma_\sigma^2/4)}, \quad (41)$$

where the momenta are defined as in Fig. 6. As the above expression contains a triple propagator it turns out to be convenient to treat it in an approximate fashion. If one makes the physically reasonable assumption that the 3-momenta of the σ mesons are about equal in magnitude to that of the exchanged pion, and that the emitted pions carry away most of the energy while the exchanged pion takes most of the 3-momentum, then one arrives at the approximations $\vec{k}_1 \approx -\vec{k}$, $\vec{k}_2 \approx \vec{k}$, $|k_1^0| \approx |k_2^0| \approx (\omega_a + \omega_b)/2$ and $k_0 \approx (\omega_b - \omega_a)/2$, which allow for a simpler treatment of the pion-exchange amplitudes. Taking also into account the crossed pion exchange term which gives an extra factor of 2, one arrives at the expression

$$\begin{aligned} T_{2q} = & -2 \cdot (8\pi\lambda)^2 \left\{ \frac{1}{3} \left(\frac{\vec{q}^2}{4} - Q_f^2 \right) [\mathcal{M}_{e1} - A^2(\mathcal{M}_{e2} - \mathcal{M}_{e3})] + \left(\frac{\vec{q}^2 z^2}{4} - \frac{2}{3} Q_f^2 - \frac{\vec{q}^2}{12} \right) \mathcal{M}_{e4} \right. \\ & \left. + \frac{\omega_a \omega_b}{4} (\omega_a - \omega_b)^2 (\mathcal{M}_{e2} - \mathcal{M}_{e3}) \right\}, \end{aligned} \quad (42)$$

which replaces eq. (34). Note that in eq. (42), the term proportional to the matrix element \mathcal{M}_{e4} originates from the term in square brackets in eq. (33), which was not included in eq. (34). The matrix elements in eq. (42) may, in the non-relativistic approximation, be expressed as

$$\mathcal{M}_{e1} = \int_0^\infty dr u_f(r) u_i(r) j_0(Q_f r) \frac{1}{4\pi} (M_\sigma^2 + \Gamma_\sigma^2/4)^2 \left(\frac{e^{-Xr}}{2X} \right), \quad (43)$$

$$\mathcal{M}_{e2} = \int_0^\infty dr u_f(r) u_i(r) j_0(Q_f r) \frac{1}{4\pi} \frac{(M_\sigma^2 + \Gamma_\sigma^2/4)^2}{(X^2 - A^2)^2} A Y_0(Ar), \quad (44)$$

$$\mathcal{M}_{e3} = \int_0^\infty dr u_f(r) u_i(r) j_0(Q_f r) \frac{1}{4\pi} \frac{(M_\sigma^2 + \Gamma_\sigma^2/4)^2}{(X^2 - A^2)^2} \left(X Y_0(Xr) + \frac{(X^2 - A^2)}{2X} e^{-Xr} \right), \quad (45)$$

$$\mathcal{M}_{e4} = \int_0^\infty dr u_f(r) u_i(r) j_2(Q_f r) \frac{1}{4\pi} \frac{(M_\sigma^2 + \Gamma_\sigma^2/4)^2}{(X^2 - A^2)^2} F_2(r). \quad (46)$$

In the above matrix elements, X is defined as $X = \sqrt{M_\sigma^2 + \Gamma_\sigma^2/4 - (\omega_a + \omega_b)^2/4}$, while $Y_0(r)$ denotes the Yukawa function e^{-r}/r . Note that when the value of k_0^2 exceeds m_π^2 , the analytic continuation $A \rightarrow -i\sqrt{k_0^2 - m_\pi^2}$ [21] is employed for the matrix element (44). Further $u_f(r)$ and $u_i(r)$ denote the reduced radial wave functions for the final and initial state heavy quarkonia, respectively. The function $F_2(r)$ is defined as

$$F_2(r) = \frac{3}{r^3} (e^{-Ar} - e^{-Xr}) + \frac{3}{r^2} (Ae^{-Ar} - Xe^{-Xr}) + \frac{1}{r} (A^2e^{-Ar} - X^2e^{-Xr}) - \frac{e^{-Xr}(X^2 - A^2)}{2} \left(\frac{1 + rX}{r} \right), \quad (47)$$

a form which is closely related to and in the limit $m_\sigma \rightarrow \infty$ actually reduces to a Yukawa Y_2 function [21]. It turns out that the matrix element (46) is numerically quite insignificant, because of the strong suppression caused by the j_2 function for small values of Qr . Also, the smallness of k_0 as compared with \vec{k} precludes the terms proportional to k_0 and k_0^2 in eq. (33) from playing any major role.

At this point, it is desirable to check the quality of the approximations made in obtaining the above matrix elements. This is possible since the triple propagator in eq. (41) may also be considered without any approximation in k_1 and k_2 , at the price of numerically much more cumbersome expressions, if one makes use of the Feynman parameterization

$$\frac{1}{ABC} = 2 \int_0^1 dx x \int_0^1 dy \frac{1}{[A(1-x) + Bxy + Cx(1-y)]^3}. \quad (48)$$

In that case, the amplitude of Fig. 6 leads to an expression which replaces eq. (34), and is of the form

$$T_{2q} = -(8\pi\lambda)^2 \left\{ \frac{1}{3} \left(\frac{\vec{q}^2}{4} - Q_f^2 \right) \left[\int_0^1 dx x \int_0^1 dy \{ \mathcal{M}_I - A^2 \mathcal{M}_{II} \} \right] + \int_0^1 dx x \int_0^1 dy \left(-\frac{\vec{q}^2}{4} (1 - 2x + xy) - Q_f^2 (1 - xy) + qQ_f z (1 - x) \right) \left(-\frac{\vec{q}^2}{4} (1 - 2x + xy) + Q_f^2 (1 - xy) + qQ_f z x (1 - y) \right) \mathcal{M}_{II} + \omega_a \omega_b k_0^2 \int_0^1 dx x \int_0^1 dy \mathcal{M}_{II} \right\} + T_{\text{exc}}, \quad (49)$$

where the matrix elements are given by

$$\mathcal{M}_I = 2 \int_0^\infty dr u_f(r) u_i(r) \frac{(M_\sigma^2 + \Gamma_\sigma^2/4)^2}{8\pi A} e^{-Ar} j_0 \left(r \sqrt{\frac{\vec{q}^2}{4} (1 - 2x + xy)^2 + Q_f^2 x^2 y^2 + qQ_f z (1 - 2x + xy) xy} \right), \quad (50)$$

$$\mathcal{M}_{II} = 2 \int_0^\infty dr u_f(r) u_i(r) \frac{(M_\sigma^2 + \Gamma_\sigma^2/4)^2}{32\pi A^3} e^{-Ar} (rA + 1) j_0 \left(r \sqrt{\frac{\vec{q}^2}{4} (1 - 2x + xy)^2 + Q_f^2 x^2 y^2 + qQ_f z (1 - 2x + xy) xy} \right). \quad (51)$$

Here the term proportional to k_0^2 is again only of minor importance. Note that in order to obtain the contribution T_{exc} to eq. (49), it is necessary to make the substitution $k_a \leftrightarrow k_b$, which implies $\omega_a \leftrightarrow \omega_b$

and $Q_f \rightarrow -Q_f$. In the above matrix elements, the quantity A is now defined as $A = \sqrt{m_*^2 - K_0^2}$, involving an effective mass m_* and an energy transfer variable K_0 . These are defined according to

$$m_*^2 = \left(M_\sigma^2 + \frac{\Gamma_\sigma^2}{4} \right) (1 - xy) - m_\pi^2 x(2(1 - x)(1 - y) - xy^2) + 2 \left(\frac{\vec{q}^2}{4} - Q_f^2 \right) x(1 - x)(1 - y), \quad (52)$$

$$K_0 = \omega_a(1 - x) - \omega_b x(1 - y) + k_0, \quad (53)$$

where M_σ again denotes the pole position $m_\sigma - i\Gamma_\sigma/2$ of the sigma resonance, and k_0 is taken to be $(\omega_b - \omega_a)/2$.

All the matrix elements for the pion exchange amplitudes have here been considered in the non-relativistic limit, even though it was noted that that limit is not realistic in case of the single quark amplitudes. The employment of the nonrelativistic limit is expected to be permissible here since the Yukawa functions which arise from the propagators of the exchanged pions and σ mesons negate the delicate orthogonality that is inherent in the wave functions plotted in Fig. 2. Thus relativistic effects constitute only a correction to the pion-exchange matrix elements, and are expected to be rather small because of the relatively large constituent masses of the charm and bottom quarks. If, however, it is desirable to consider relativistic effects for the pion-exchange amplitudes, a relativistic matrix element analogous to eq. (37) may be constructed according to

$$\mathcal{M}_{\text{exch}}^{\text{rel}} = \int \frac{d^3 P}{(2\pi)^3} \frac{d^3 k}{(2\pi)^3} \varphi_f^* \left(\vec{P} + \frac{\vec{Q}}{2} - \frac{\vec{k}}{2} \right) T_{2q}(\vec{k}, \vec{P}) \varphi_i \left(\vec{P} - \frac{\vec{Q}}{2} + \frac{\vec{k}}{2} \right), \quad (54)$$

where the amplitude $T_{2q}(\vec{k}, \vec{P})$ corresponds to eq. (32) multiplied by the σ factors from eq. (35) and subject to the approximations that led to eq. (42). Furthermore, $T_{2q}(\vec{k}, \vec{P})$ should also contain the quark and antiquark bispinors analogous to eq. (38). In the matrix element (54), the wavefunctions are defined according to

$$\varphi_f^* = \int d^3 r' e^{i(\vec{P} + \frac{\vec{Q}}{2} - \frac{\vec{k}}{2}) \cdot \vec{r}'} \varphi_f^*(\vec{r}'), \quad (55)$$

$$\varphi_i = \int d^3 r e^{-i(\vec{P} - \frac{\vec{Q}}{2} + \frac{\vec{k}}{2}) \cdot \vec{r}} \varphi_i(\vec{r}). \quad (56)$$

Numerical evaluation and comparison of the approximate model for the pion exchange diagrams with the version based on the Feynman parameterization (48) indicates that the approximate model successfully describes the pion exchange amplitudes, with only very small deviations from eq. (49). To summarize, a very good description of the pion exchange diagrams may already be obtained by considering only the first term in eq. (42). The results presented in the next section correspond, unless otherwise indicated, to eq. (36) for the single quark amplitudes, and to eq. (42) with exception of the term proportional to k_0^2 for the pion exchange amplitudes.

4 Results for $\Upsilon' \rightarrow \Upsilon \pi\pi$ and $\psi' \rightarrow J/\psi \pi\pi$

The pion exchange mechanisms in eq. (29) may *a priori* give large contributions to the decays $\Upsilon' \rightarrow \Upsilon \pi\pi$ and $\psi' \rightarrow J/\psi \pi\pi$ because they are not suppressed by the orthogonality of the $2S$ and $1S$ wave functions of the heavy quarkonium states. Therefore, the contribution from the pion exchange diagrams is expected to be dominant if point couplings to heavy quarks are employed. This is illustrated in Fig. 10, where the case of $m_\sigma = \infty$ corresponds to pointlike couplings. Also, if the $\pi\pi$ decay of heavy quarkonium states is dominated by pion exchange mechanisms, the widths of the bottomonium states are expected to be larger than those of the corresponding charmonium states, which is in conflict with experiment [1, 2]. This is the case because of the narrowness of the $b\bar{b}$ wavefunctions combined with the short range nature of the Yukawa functions in the pion exchange amplitude. This suggests that the $Q\pi\pi$ coupling is mediated by a light scalar meson or glueball.

Indeed, if a σ meson lighter than 1 GeV is employed in combination with a relativistic treatment of the single quark amplitudes in eq. (29), then the effects of pion exchange diagrams may be reduced, and their contributions may in fact become subdominant as compared to the single quark amplitudes, which allows agreement with experiment. The results presented in this section indicate that σ masses of the order ~ 500 MeV lead to a favorable description of the current experimental data on the $\pi\pi$ decays of the $2S$ states of heavy quarkonia.

The calculated widths and two-pion energy distributions were obtained by simultaneously optimizing the results for $\Upsilon' \rightarrow \Upsilon \pi^+\pi^-$ and $\psi' \rightarrow J/\psi \pi^+\pi^-$. Furthermore, even though the coupling constant λ is in principle a free parameter, it is strongly constrained by the shape of the $\pi\pi$ energy distribution. This reflects the fact that the pion-exchange amplitudes may contribute significantly alongside the single quark diagrams. It is therefore necessary to choose λ in such a way that not only the width but also the $\pi\pi$ energy spectrum is optimally described.

The results, which yielded the σ meson parameters $m_\sigma = 450$ MeV and $\Gamma_\sigma = 550$ MeV, are shown in Figs. 7 and 8 for negative and positive values of λ , respectively. The calculated decay widths corresponding to $\lambda = -0.02$ are shown Table 3. This negative value of λ was found to lead to an optimal description of both the $b\bar{b}$ and $c\bar{c}$ data. It is noteworthy that the sensitivity to the sign of λ is entirely due to the presence of pion exchange amplitudes in eq. (29). The masses of the heavy quarkonium states correspond to those given by ref. [1]. Using instead the energy eigenvalues of Table 1 corresponding to the wave functions obtained by solving the BSLT equation makes very little difference since they agree quite well with the experimental masses. The pion masses were taken to be 139.57 MeV for the charged pions, and 134.98 MeV for the neutral pion. The heavy constituent quark masses used were those listed in Table 2. Unless otherwise indicated, the results in this section refer to $\pi^+\pi^-$ decays.

Decay	Γ_{tot}	Br.Rat.	Γ_{exp}	Γ_{calc}	q_{max}
$\Upsilon' \rightarrow \Upsilon \pi^+\pi^-$	44 ± 7 keV	18.8 ± 0.6 %	8.3 ± 1.3 keV	5.89 keV	475 MeV
$\Upsilon' \rightarrow \Upsilon \pi^0\pi^0$		9.0 ± 0.8 %	4.0 ± 0.8 keV	3.07 keV	480 MeV
$\psi' \rightarrow J/\psi \pi^+\pi^-$	277 ± 31 keV	31.0 ± 2.8 %	86 ± 12 keV	53.5 keV	477 MeV
$\psi' \rightarrow J/\psi \pi^0\pi^0$		18.2 ± 2.3 %	50 ± 10 keV	27.8 keV	481 MeV

Table 3: Experimental data and calculated widths for $\pi\pi$ decays of the Υ' and ψ' mesons, for $\lambda = -0.02 \text{ fm}^3$, $m_\sigma = 450$ MeV and $\Gamma_\sigma = 550$ MeV. Experimental total widths, branching fractions and resulting widths for $\pi^+\pi^-$ and $\pi^0\pi^0$ are given. The column q_{max} lists the maximal momenta $|\vec{q}|$ attainable by the pion pairs.

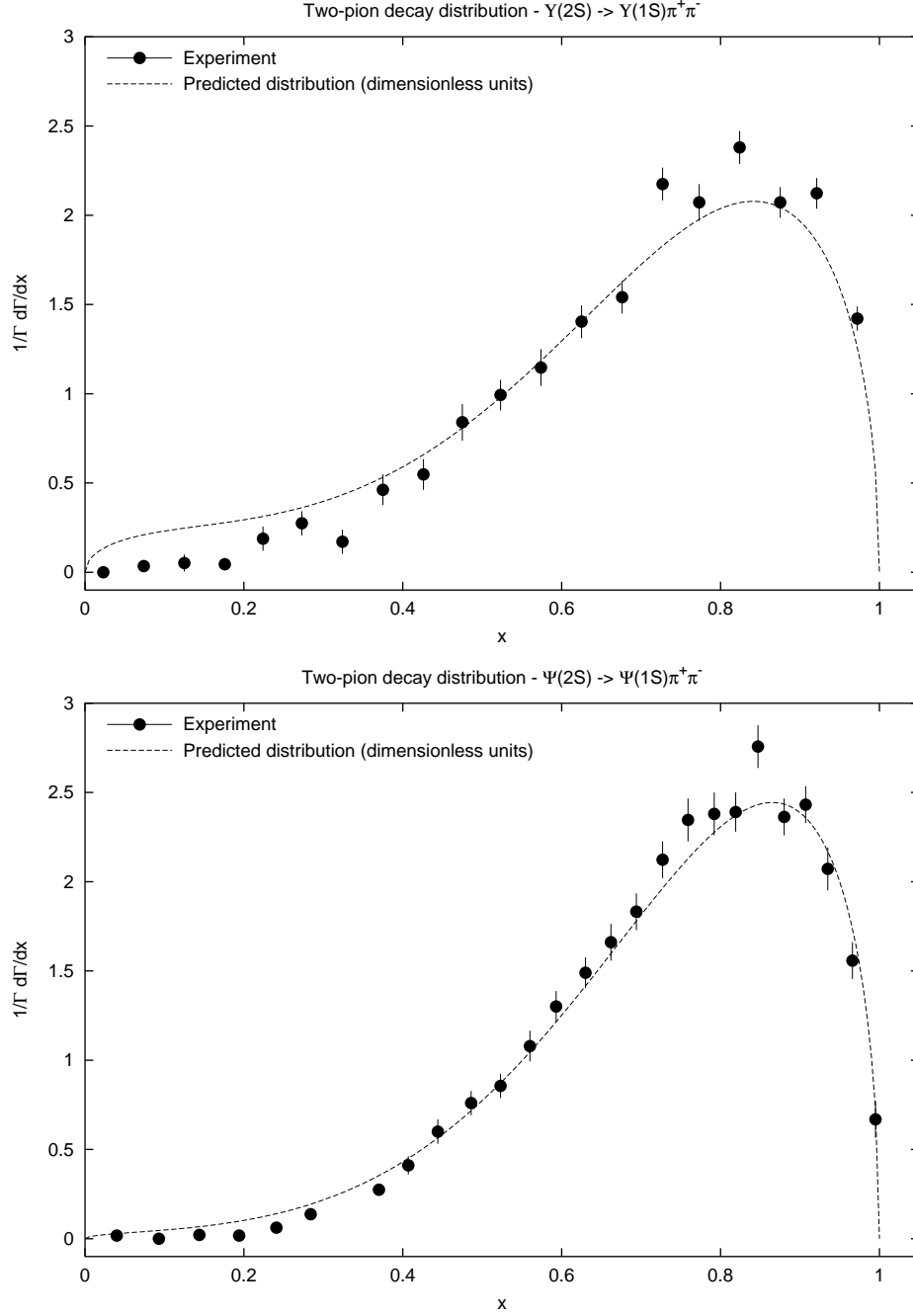


Figure 7: Comparison of calculated and experimental [2] $\pi\pi$ energy distributions for $\Upsilon' \rightarrow \Upsilon\pi^+\pi^-$ and $\psi' \rightarrow J/\psi\pi^+\pi^-$. The calculated distributions correspond to $m_\sigma = 450$ MeV and $\Gamma_\sigma = 550$ MeV and $\lambda = -0.02 \text{ fm}^3$. The calculated widths for decay by charged pions is 5.89 keV for $b\bar{b}$ and 53.5 keV for $c\bar{c}$.

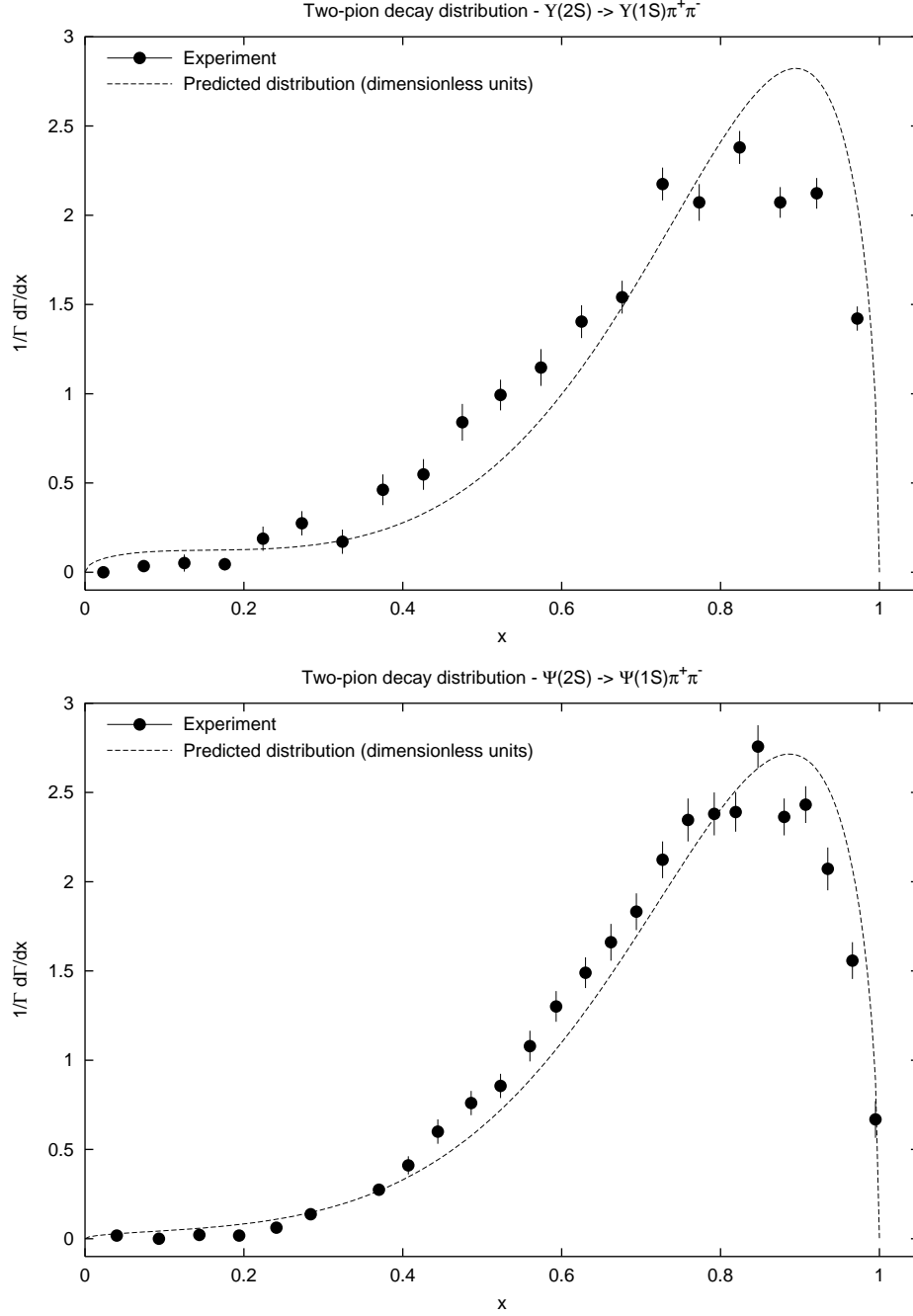


Figure 8: Comparison of calculated and experimental [2] $\pi\pi$ energy distributions for $\Upsilon' \rightarrow \Upsilon\pi^+\pi^-$ and $\psi' \rightarrow J/\psi\pi^+\pi^-$. The calculated distributions correspond to $m_\sigma = 450$ MeV and $\Gamma_\sigma = 550$ MeV and $\lambda = +0.02 \text{ fm}^3$. The calculated widths for decay by charged pions is 9.54 keV for $b\bar{b}$ and 67.5 keV for $c\bar{c}$.

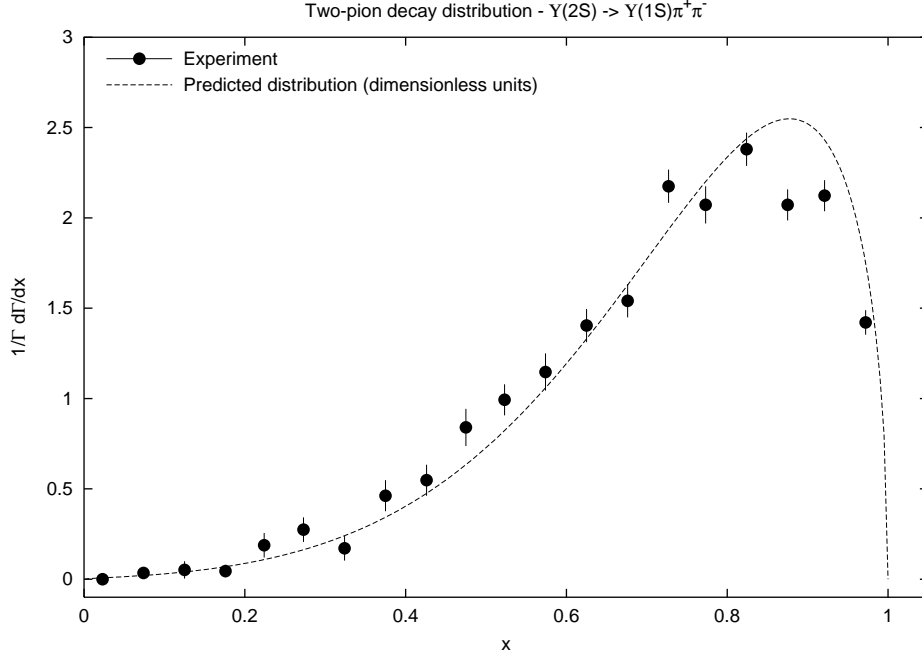


Figure 9: Comparison of calculated and experimental [2] $\pi\pi$ energy distributions for $\Upsilon' \rightarrow \Upsilon \pi^+ \pi^-$, with $m_\sigma = 450$ MeV, $\Gamma_\sigma = 550$ MeV and $|\lambda| = 0.02 \text{ fm}^3$. The calculated $\pi^+ \pi^-$ width is 7.09 keV. This result is obtained when only the single quark diagrams are retained in the calculations.

The results presented in Figs. 7 and 8 indicate that a more favorable description of the $\pi\pi$ invariant mass distributions may be obtained if the coupling constant λ is taken to be negative. This appears to be in line with the fact that the experimental distributions for $b\bar{b}$ and $c\bar{c}$ as shown in Figs. 7 and 8 show slight differences. In particular, the peak at high x is somewhat lower for $b\bar{b}$, while the tail at low x is broader for $b\bar{b}$. It has also been noted in ref. [2] that the resonance model of ref. [5] cannot be simultaneously fitted to both the $b\bar{b}$ and $c\bar{c}$ decay distributions. It is seen from Fig. 7 that if negative values of λ are employed then the abovementioned qualitative differences between the $b\bar{b}$ and $c\bar{c}$ decay distributions may be accounted for. The obtained value for the σ meson mass, 450 MeV, is constrained even if single quark diagrams only are considered. In that case, a higher σ mass would lead to a distribution which is peaked too far to the right. If pion exchange amplitudes are considered as well, a higher σ mass leads to unrealistically large pion exchange contributions. The results are not very sensitive to the σ width, but standard values of ~ 500 MeV appear to be favored by the calculations.

It is also evident from Fig. 7 that the pion exchange contribution, while having an overall favorable effect, appears to be somewhat overpredicted, particularly for $b\bar{b}$. This problem can be traced to the nonrelativistic treatment of the pion exchange contribution, and can be alleviated if relativistic matrix elements are employed according to eq. (54). This relativistic weakening of the pion exchange amplitudes may also remedy the apparent underprediction of the $\Upsilon' \rightarrow \Upsilon \pi^+ \pi^-$ width as given by Table 3. For $c\bar{c}$ the results are much less sensitive to the exact strength and form of the pion exchange amplitude, an effect which is due to the much broader radial wavefunctions of the $c\bar{c}$ states. In case of the decay $\psi' \rightarrow J/\psi \pi^+ \pi^-$, it may actually be desirable to employ a 20 – 30 % larger value of λ , as indicated e.g. in ref. [6].

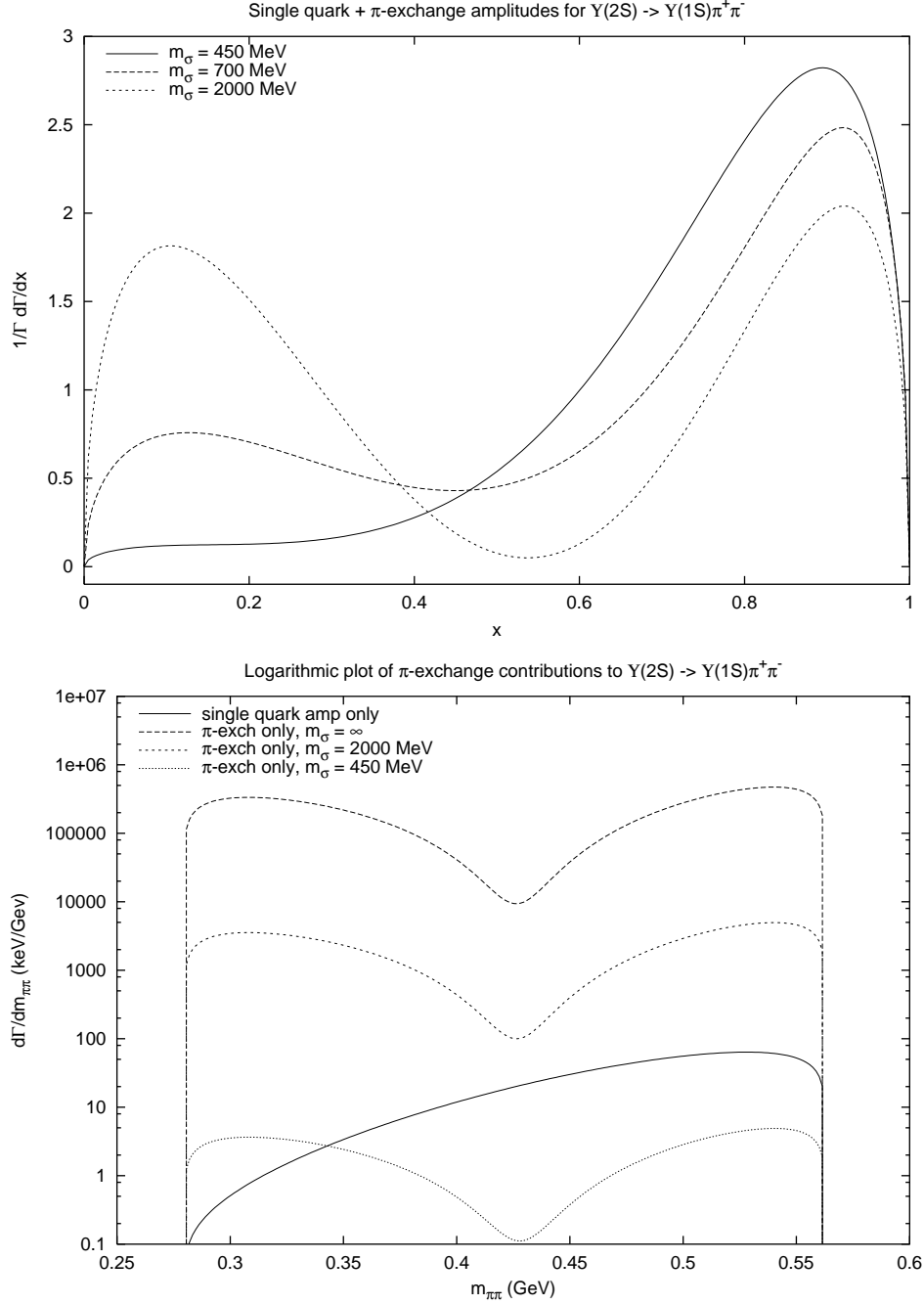


Figure 10: Illustration of the reduction of π -exchange amplitudes brought about by the introduction of an intermediate σ meson with a width of $\Gamma_\sigma = 550$ MeV, and $\lambda = +0.02 \text{ fm}^3$. Note that the relativistic single quark amplitude (37) begins to dominate when m_σ is less than ~ 1 GeV.

As expected, the logarithmic plot of the pion exchange amplitudes in Fig. 10 reveals that if point couplings between heavy constituent quarks and two-pions are employed, then pion exchange will be the dominant mechanism for $\pi\pi$ decay of the heavy quarkonium states. Fig. 10 also shows that for the values of m_σ obtained by fitting the model to experimental data, the pion exchange amplitudes are subdominant and constitute a relatively small correction. However, the contribution from pion exchange may still not be neglected. By comparing Figs. 7 and 8, it is revealed that negative values of λ allow for better agreement with experiment.

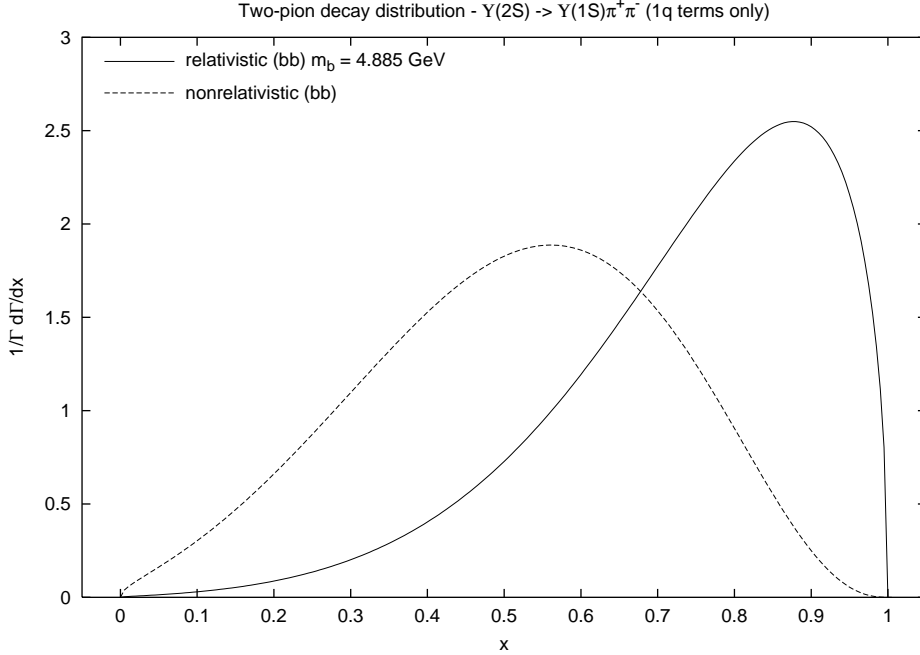


Figure 11: Comparison between relativistic and nonrelativistic results for bottomonium ($b\bar{b}$), when only the single quark amplitudes are considered. The results correspond to a σ mass of 450 MeV and width of 550 MeV, and a coupling constant of $|\lambda| = 0.02$. The relativistic and nonrelativistic forms give $\pi^+\pi^-$ widths of 7.09 keV and 0.47 keV, respectively. In case of charmonium ($c\bar{c}$), the nonrelativistic distribution is qualitatively similar, but somewhat shifted to the right.

Fig. 11 illustrates the fact that, even though the charm and bottom constituent quarks are heavy, the nonrelativistic limit is not applicable for the single quark diagrams. This comes about because of the orthogonality of the wavefunctions in the matrix element (40). It follows that the single quark mechanisms are highly suppressed since the product qr is always small for the observables considered here. If the spinor factors of eq. (38) in the relativistic matrix element (37) are taken into account, they will lead to an increase of the contributions from single quark diagrams. The resulting amplitude then becomes almost constant over the whole range of two-pion momenta covered by the $\Upsilon' \rightarrow \Upsilon\pi\pi$ decays, allowing agreement with the phenomenological deductions of earlier work [5, 6]. Also, since the relativistic modifications increase the effect of the single quark amplitudes by a factor ~ 10 , they also allow avoidance of large values of the coupling constant λ . This is even more important since otherwise, even though the pion exchange contributions are very much suppressed by inclusion of the σ meson, they may still overwhelm the single quark contributions in the nonrelativistic limit, making it very difficult

to obtain agreement with the experimental $\pi\pi$ energy distributions. It is worth noting in this context that the nonrelativistic approximation becomes realistic only if the constituent quark mass is larger than ~ 30 GeV.

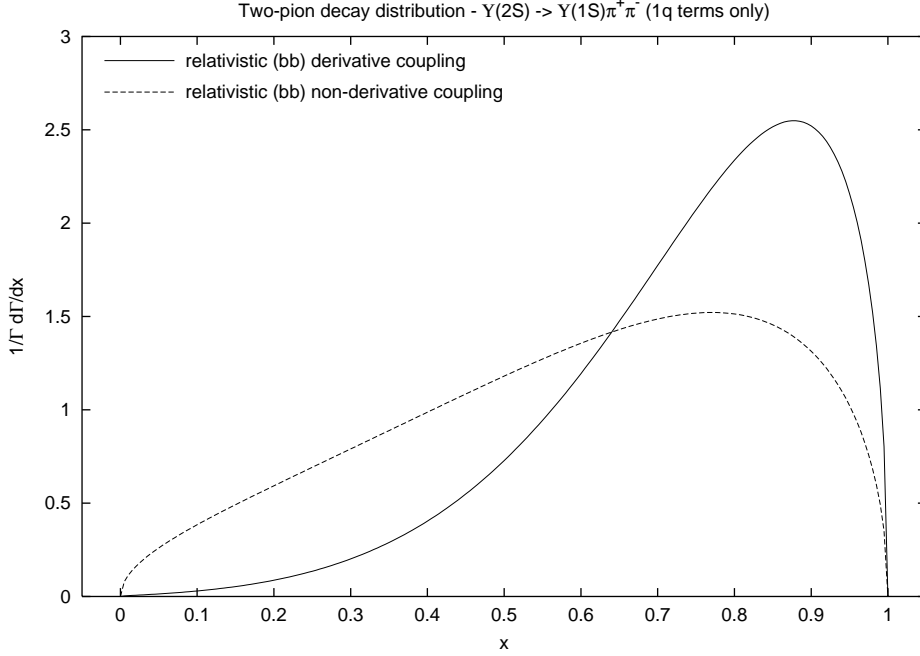


Figure 12: Comparison between derivative and non-derivative couplings in the relativistic case (single quark diagrams only) for $b\bar{b}$. The results correspond to the same set of parameters as Fig. 11.

Another interesting point is to check whether the derivative coupling to pions in eq. (28) actually does provide a superior description of the $\pi\pi$ energy spectrum. A comparison between a model with derivative couplings and one without them is given for the single quark amplitudes in Fig. 12. As the inclusion of the σ mesons leads to the same conclusions of the vanishing of the pion exchange contributions for both models, a fair comparison may already be obtained by comparing the single quark amplitudes only. Fig. 12 indicates that even in the relativistic case, a model without derivative couplings on the pion fields does not provide a good description of the $\pi\pi$ distribution. Such a model is seen to give a rather structureless distribution, which does not reproduce the sharp peak at large values of the scaled $\pi\pi$ invariant mass x and also gives a wrong curvature at low x , a result which has also been obtained by ref. [5]. This is reassuring since the derivative couplings for pions are consistent with the role of pions as Goldstone bosons of the spontaneously broken approximate chiral symmetry of QCD.

5 Discussion

The results of the previous section indicate that an overall satisfactory description of the decays $\Upsilon' \rightarrow \Upsilon \pi\pi$ and $\psi' \rightarrow J/\psi \pi\pi$ has been achieved. This good agreement was shown to depend on several factors, most notably the use of derivative couplings to pions, relativistic treatment of amplitudes where the two-pions are emitted from a single constituent quark, and the inclusion of an intermediate scalar σ meson with a mass of ~ 500 MeV. Inclusion of the σ meson has been shown to lead to a drastic reduction of the amplitudes, where one of the emitted pions is rescattered by the other constituent quark. Still, there remains some issues with these transitions that deserve further discussion.

As seen from Table 3, the decay widths for the $c\bar{c}$ system are generally underpredicted by $\sim 30-40\%$, if the coupling constant λ is determined from the corresponding decays in the $b\bar{b}$ system. There appears to be no obvious reason for this underprediction, as the results are not exceedingly sensitive to the particulars of the model used, nor to the exact values of the masses of the constituent quarks involved. Furthermore, the pion exchange amplitudes are relatively insignificant for the $c\bar{c}$ system, and cannot account for this underprediction. If the value of λ is increased by $\sim 20\%$ for the $c\bar{c}$ system, the computed width for the transition $\psi' \rightarrow J/\psi \pi^+\pi^-$ comes into close agreement with the current experimental data. A similar requirement for a slight increase of the coupling constant for the $c\bar{c}$ system has also been noted by ref. [6], and is therefore likely to be a real effect. Nevertheless, it has to be noted that the total width of the ψ' [1] state is difficult to determine experimentally and still remains somewhat uncertain.

It is also noteworthy that the agreement between the calculated and experimental $\pi\pi$ energy distributions, as shown in Fig. 7, turns out to be somewhat better for $c\bar{c}$ than for $b\bar{b}$. A likely explanation for this feature is the nonrelativistic treatment of the pion exchange amplitudes, eq. (42). This results in a slight overprediction of the pion exchange contribution, the effect of which is amplified by the narrowness of the $b\bar{b}$ wavefunctions. As the present model has only few degrees of freedom, and does not really constitute a "fit" to the available data (e.g. the quark masses are fixed by the $Q\bar{Q}$ spectrum) then lack of perfect agreement with experiment is not unexpected. A somewhat better fit to the available data on $\pi\pi$ decay in the $c\bar{c}$ and $b\bar{b}$ systems has been obtained in ref. [6] by employment of a more complex Lagrangian with more adjustable coupling constants. Another possible explanation is that eq. (35) may only be a very crude model for the interacting $\pi\pi$ state. Indeed, ref. [5] has employed a somewhat more sophisticated σ model where the width of the resonance is not a constant. A further possibility is that two-quark contributions associated with intermediate negative energy quarks (see e.g. the "Z" diagrams of ref. [20]) may significantly modify the calculated decay distributions and widths. These effects, which depend explicitly on the form and Lorentz coupling structure of the quark-antiquark interaction arise from the elimination of negative energy components in the BSLT quasipotential reduction, which has been employed in this work. For e.g. the scalar confining interaction and the coupling (28) they can be shown to be proportional to M_Q^{-3} at the nonrelativistic limit and are therefore highly relativistic effects that, when treated properly, are expected to be of minor significance.

An outstanding problem with the hadronic decays of heavy quarkonia has been the theoretical understanding of the $\Upsilon(3S) \rightarrow \Upsilon \pi\pi$ and $\Upsilon(3S) \rightarrow \Upsilon' \pi\pi$ decays. These have been experimentally studied in ref. [22], and were found to have roughly equal widths of ~ 1 keV. This is a problematic feature since the derivative coupling of the pions in combination with the phase space factors naturally lead to a strong suppression of the latter decay mode relative to the former. This has led to the introduction of different coupling constants for the different decay modes in order to compensate for the increase or decrease in phase space. While this may be reasonable if the Υ and ψ states are treated as fundamental particles, it is difficult to formulate a consistent model using variable coupling constants if the $\pi\pi$ decay is modeled in terms of a $Q\pi\pi$ coupling. Despite the generally good agreement with experiment obtained for the $\pi\pi$ decays of the Υ' and ψ' states, a width of only 1 keV for $\Upsilon(3S) \rightarrow \Upsilon \pi\pi$ cannot be achieved with the present set of parameters.

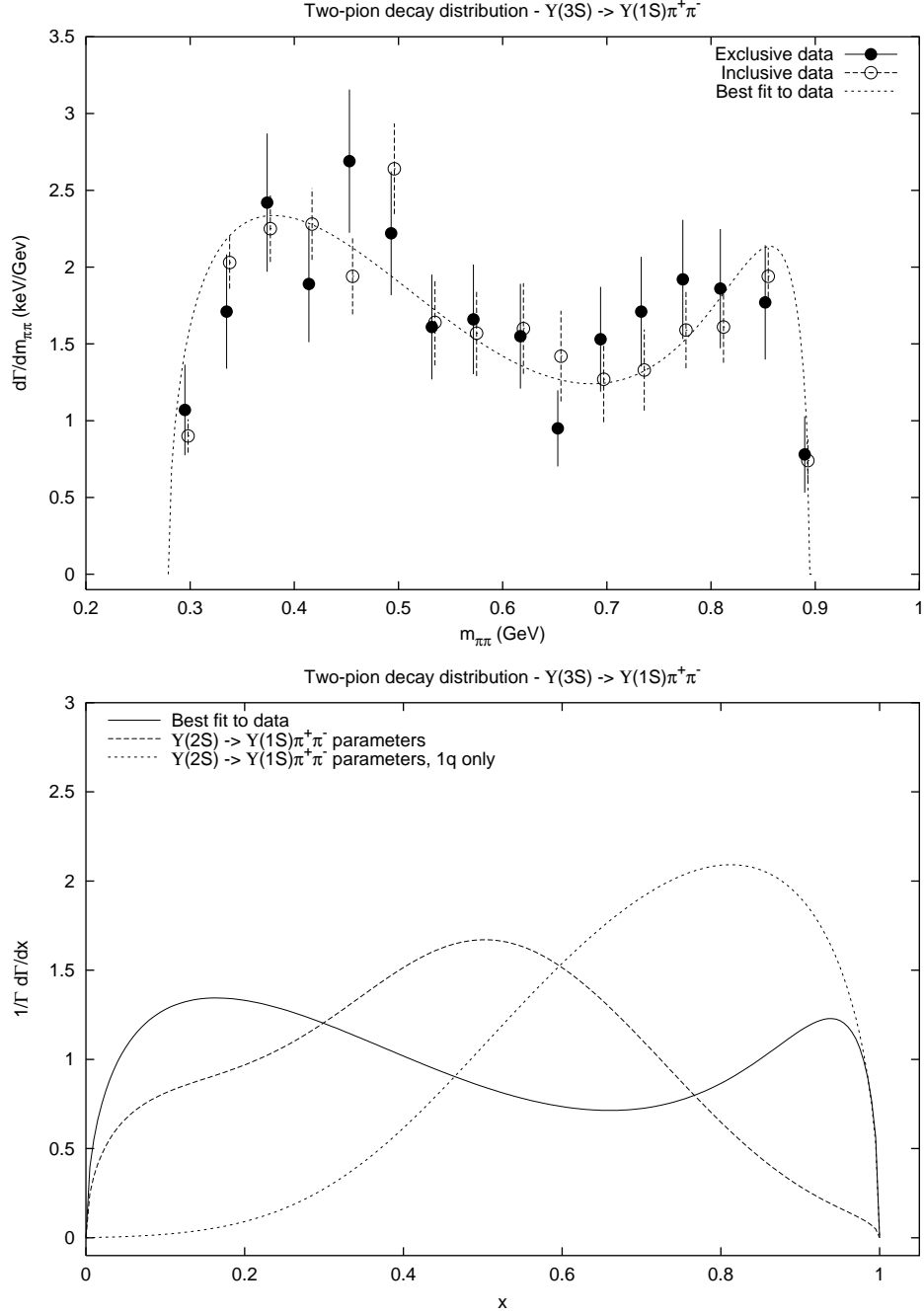


Figure 13: Best fit to experimental data [22] for the decay $\Upsilon(3S) \rightarrow \Upsilon \pi^+ \pi^-$ and comparison with results obtained using the parameters from Table 3. The best fit parameters obtained were $m_\sigma = 1400$ MeV, $\Gamma_\sigma = 100$ MeV, $\lambda = 2.7 \cdot 10^{-3}$, and give $\Gamma_{\pi^+ \pi^-} = 1.07$ keV.

The $\pi\pi$ energy distribution of the $\Upsilon(3S) \rightarrow \Upsilon \pi\pi$ decay shows an anomalous double-peaked structure, which cannot be explained by models dominated by single-quark amplitudes, such as the one employed above for the $\pi\pi$ decays of the Υ' and ψ' states. This is in obvious contradiction with the conclusions from analysis of the $\pi\pi$ energy distributions of the $\Upsilon' \rightarrow \Upsilon \pi\pi$ decays. In this situation it seems natural to assume that the initial $\Upsilon(3S)$ state may have a more complex structure than a simple radial excitation of the $\Upsilon(1S)$. This has been investigated in refs. [23, 24], where acceptable agreement with the experimentally observed $\pi\pi$ energy distributions has been attained by consideration of intermediate $B\bar{B}^*$ states. However, the explicit calculation of coupled channel effects in ref. [25], indicates that the interpretation suggested by refs. [23, 24] may not be valid. However, the model of ref. [25] also fails to reproduce the experimentally observed $\pi\pi$ spectrum.

The results obtained when the energy distribution for the decay $\Upsilon(3S) \rightarrow \Upsilon \pi^+\pi^-$ is calculated with the same model as that employed for the $\Upsilon' \rightarrow \Upsilon \pi^+\pi^-$ decay are shown in Fig. 13. The width so obtained is large, 20.1 keV, mainly because the $\pi\pi$ momentum $|\vec{q}|$ may extend to over 800 MeV, and the form of the distribution does not agree with the experimentally determined double-peaked structure. However, if only single quark diagrams are considered, the calculated distribution does appear quite similar to that obtained in ref. [26], where $\pi\pi$ final state interactions have been taken into account. In that case the width is obtained here as 25.1 keV.

However, it is interesting to see what may be learned by using models of the present type to fit the observed double-peaked structure of the $\Upsilon(3S) \rightarrow \Upsilon \pi^+\pi^-$ energy spectrum. In this case there are three parameters (λ , m_σ and Γ_σ) that may be used as free parameters. It turns out, that the present model does in fact have sufficient freedom to accommodate a double-peaked $\pi\pi$ energy distribution, as may be seen from Fig. 13. An optimal description of the $\pi\pi$ distribution is obtained for the parameter values $m_\sigma = 1400$ MeV, $\Gamma_\sigma = 100$ MeV, $\lambda = 2.7 \cdot 10^{-3}$, and gives $\Gamma_{\pi^+\pi^-} = 1.07$ keV. Since the employed scalar meson is now much heavier, the contributions from the pion exchange and single quark amplitudes are of equal magnitude, which makes it possible to obtain a double-peaked spectrum. This scalar meson mass falls within the range of the empirical scalar resonances $f_0(1370)$ with mass 1200-1500 MeV and a width of 200-500 MeV, and $f_0(1500)$ with mass 1500 ± 10 MeV and a width of 112 ± 10 MeV [1]. Both of these states have, analogously to the σ , a strong coupling to $\pi\pi$. As a relativistic treatment of the pion exchange amplitudes will weaken their contribution slightly, the $f_0(1500)$ appears to be favored by this phenomenological analysis. Since most parts of the present model are concerned with the $\sigma\pi\pi$ coupling, an explanation for the apparent absence of an intermediate σ meson in case of the decay $\Upsilon(3S) \rightarrow \Upsilon \pi^+\pi^-$ may possibly be found in the (nonperturbative) hadronization of the gluon pair emitted by the heavy constituent quark.

Finally, it is worth noting that the $\pi\pi$ energy distribution for the decay $\Upsilon(3S) \rightarrow \Upsilon' \pi^+\pi^-$ is not of decisive importance since the maximum value of $|\vec{q}|$ is only ~ 170 MeV for that decay mode. This implies that the shape of the decay distribution is mostly determined by phase space alone, and cannot be used to discriminate between different theoretical models. The experimental data obtained by ref. [22] is also rather crude for that decay. If the parameters given in Table 3 are employed, the $\pi\pi$ width for the transition $\Upsilon(3S) \rightarrow \Upsilon' \pi^+\pi^-$ comes to ~ 0.02 keV, which is much smaller than the empirically determined 0.7 ± 0.2 keV. This fact was also noted by ref. [6], where it was found that a much larger coupling constant had to be employed. The shape of the $\pi\pi$ distribution is however very insensitive to the σ parameters, and can be fitted with almost any values.

Acknowledgments

We thank Ted Barnes for pointing out the interest in $\pi\pi$ decays of heavy quarkonia, and Dmitri Kharzeev for an instructive discussion. TL thanks the Waldemar von Frenckell foundation for a fund grant. Research supported in part by the Academy of Finland through grant No. 43982.

References

- [1] D.E. Groom *et al.*, Eur. Phys. J. **C15** (2000) 1 (Particle Data Group)
- [2] ARGUS Coll. (H. Albrecht *et al.*), Z. Phys. **C35:283** (1987)
- [3] J.-W. Chen and M.J. Savage, Phys. Rev. **D57:2837** (1998) hep-ph/9710338
- [4] V.A. Novikov and M.A. Shifman, Z. Phys. **C8:43** (1981)
- [5] J. Schwinger *et al.*, Phys. Rev. **D12:2617** (1975)
- [6] T. Mannel and R. Urech, Z. Phys. **C73:541** (1997) hep-ph/9510406
- [7] R. Blankenbecler and R. Sugar, Phys. Rev. **142** (1966) 1051
- [8] A.A. Logunov and A.N. Tavkhelidze, Nuovo Cimento **29** (1963) 380
- [9] T.A. Lähde, C.J. Nyfält and D.O. Riska, Nucl. Phys. **A674** (2000) 141, hep-ph/9908485
- [10] S. Chernyshev, M.A. Nowak and I. Zahed, Phys. Lett. **B350**, 238 (1995) hep-ph/9409207
- [11] S. Chernyshev, M.A. Nowak and I. Zahed, Phys. Rev. **D53**, 5176 (1996) hep-ph/9510326
- [12] T.A. Lähde, C.J. Nyfält and D.O. Riska, Nucl. Phys. **A645** (1999) 587, hep-ph/9808438
- [13] K.O.E. Henriksson *et al.*, Nucl. Phys. **A686** (2001) 355, hep-ph/0009095
- [14] J.L. Goity and W. Roberts, Phys. Rev. **D60:034001** (1999), hep-ph/9809312
- [15] G.S. Bali, K. Schilling and A. Wachter, Phys. Rev. **D56:2566**, (1997) hep-lat/9703019
- [16] C. Davies, eprint hep-ph/9710394
- [17] A.C. Mattingly and P.M. Stevenson, Phys. Rev. **D49:437** (1994) hep-ph/9307266
- [18] J. Zeng, J.W. Van Orden and W. Roberts, Phys. Rev. **D52**, 5229 (1995) hep-ph/9412269
- [19] S. Godfrey and N. Isgur, Phys. Rev. **D32:189** (1985)
- [20] T.A. Lähde and D.O. Riska, Nucl.Phys. **A693** (2001) 755, hep-ph/0102039
- [21] J. Chai and D.O. Riska, Nucl.Phys. **A338** (1980), 349
- [22] F. Butler *et al.*, Phys. Rev. **D49:40** (1994)
- [23] H.J. Lipkin and S.F. Tuan, Phys. Lett. **B206**, 349 (1988)
- [24] P. Moxhay, Phys. Rev. **D39:3497** (1989)
- [25] H.-Y. Zhou and Y.-P. Kuang, Phys. Rev. **D44:756** (1991)
- [26] G. Bélanger, T. DeGrand and P. Moxhay, Phys. Rev. **D39:257** (1989)